PNAS
www.pnas.org

Supplementary Information for

Reversible mitophagy drives metabolic suppression in diapausing beetles

Jacqueline E. Lebenzon*, Peter W. Denezis, Lamees Mohammad, Katherine E. Mathers, Kurtis F. Turnbull, James F. Staples and Brent J. Sinclair

Department of Biology, University of Western Ontario, London, Ontario, Canada, N6A 5B7

*Correspondence to Jacqueline E. Lebenzon

Email: jlebenzo@uwo.ca

This PDF file includes:

Materials & Methods
Figures S1 to S7
Tables S1 and S2
Legends for Datasets S1 and S2

Other supplementary materials for this manuscript include the following:

Datasets S1 (.xlsx) and S2 (.p)

Materials & Methods

Insect care and diapause induction

We established a colony of *Leptinotarsa decemlineata* with individuals originally collected from potato fields at the London Research and Development Centre in London, Ontario, Canada and maintained the colony in greenhouses at the University of Western Ontario. The population was supplemented annually with c. 50 field-collected individuals to reduce inbreeding. For general rearing (control, non-diapausing beetles), we maintained eggs, larvae, and adults on fresh Kennebec potato plants in BugDorms (Megaview science, Talchung, Taiwan, W60 × D60 × H60 cm) at 24 °C under a long daylength (16:8 L:D). We allowed adults to freely mate and lay eggs on plants in the BugDorms.

We induced diapause following Lebenzon et al., 2021 (1). Briefly, we reared eggs laid by control adults on excised potato leaves in Petri dishes lined with moist paper towel in temperature and light-controlled incubators (Sanyo Scientific, Bensenville, IL, USA) at 24 °C and short days (8:16 L:D). We transferred newly hatched larvae to 500 mL plastic containers lined with moistened paper towels and fed them daily with fresh potato leaves. We maintained larvae in groups of c. 20 in these containers until they reached the 4^{th} instar stage. We transferred 4^{th} instar larvae to 14 L plastic pupation bins filled with soil and provided them fresh leaves daily until the larvae burrowed into the soil to pupate. Once adults emerged from the soil, we transferred them to fresh plastic bins filled with soil and kept them at 15 °C (8:16 L:D), which we refer to as diapause-inducing conditions. We kept 20-30 beetles in each bin and fed these diapause-destined adults fresh potato leaves daily for 3-4 weeks after which they stopped eating and burrowed into the soil. We did not observe any females laying eggs in these diapause-destined populations. After nine weeks in diapause-inducing conditions, all beetles had burrowed into the soil. After 15-20 weeks in diapause-inducing conditions, beetles spontaneously emerged from the soil.

Whole-animal respirometry

We tracked whole-animal metabolic rate in control beetles and in beetles exposed to diapause-inducing conditions throughout their diapause programme using Sable Systems flow-through respirometry (Sable Systems International, Las Vegas, NV, USA). We included beetles from the following groups: non-diapause (control), exposed to diapause-inducing conditions for three, six, nine, 12, 15, and 20 weeks (emerged). We measured CO_2 production as a proxy for metabolic rate at 15 °C according to Williams et al., 2012 (2). Briefly, we passed dry CO_2-free air through chambers at 80 mL min^{-1} using mass-flow valves (Sierra Instruments, Monterey, California, USA) and a mass-flow controller (Super Systems Inc., Cincinnati, OH, USA). We recorded CO_2 release for 30 min per individual using a Li7000 infrared gas analyzer (LiCor, Lincoln, Nebraska, USA). We recorded data on Expedata software using a UI2 interface (Super Systems Inc., Cincinnati, OH, USA), and corrected CO_2 release to baseline recordings of an empty chamber made for 5 min before and after each run. We calculated $\dot{V}CO_2$ for three consecutive cycles of discontinuous gas exchange using the equation:

$$\dot{V}CO_2 = \left(\frac{CO_2}{1000000}\right) \times FR$$

where FR is the incurrent flow rate of CO_2-free air (mL min^{-1}) and CO_2 is the CO_2 concentration leaving the chamber (ppm). We weighed individuals before and after each run, and corrected $\dot{V}CO_2$ for body mass by dividing $\dot{V}CO_2$ by the average mass of each individual. We fasted non-diapausing beetles 24 h before measurements to ensure steady state resting metabolic rates, however we did not fast diapausing beetles because they were no longer actively feeding. We compared $\dot{V}CO_2$ measurements using a one-way ANCOVA, with beetle mass (averaged between the start and end of each run for each individual) as a co-variate, and analysed differences among treatment groups using a Tukey's HSD in R (R, version 3.3.2, R Core Team, Vienna, Austria).

High resolution respirometry

We measured mitochondrial respiration rates in saponin-permeabilized beetle flight muscle using high-resolution respirometry. We included beetles from the following groups: non-diapause (control), exposed to diapause-inducing conditions for three, six, nine, 12, 15, and 20 weeks (Emerged). From each group, we dissected thorax flight muscle directly into a 500 µl aliquot of ice-cold BIOPS permeabilization buffer (50 mM K-MES, 7.23 mM EGTA, 2.77 mM Ca_3K_2EGTA, 20 mM imidazole, 20 mM taurine, 5.7 mM ATP, 14.3 mM phosphocreatine, 6.56 mM $MgCl_2$, pH 7.1) to preserve the energetic state of the tissue (3). We removed any adhering fat body tissue while the tissue was submerged in BIOPS and placed the remaining flight muscle into 2 mL of fresh ice cold BIOPS containing 50 µg/mL of saponin (Sigma). We incubated the samples in saponin for 30 minutes on a shaker under constant agitation (300 rpm) to permeabilize the muscle fibers, and then gently transferred the permeabilized fibers to 2 mL of ice-cold mitochondrial respiration buffer (MiR05; 105 mM K-MES, 30 mM KCl, 1 mM EGTA, 10 mM KH_2PO_4, 5 mM $MgCl_2$, 5 mg/mL BSA, pH 7.1) (4), and incubated the fibers on a shaker under constant agitation for 5 minutes (300 rpm). We repeated this step twice to remove any residual saponin. Immediately after the second wash in MiR05, we gently blotted the flight muscle samples twice with a cotton swab to remove excess buffer, and weighed them on a microbalance (MX5, Mettler Toledo).

Immediately after weighing the permeabilized tissue, we gently transferred it to chambers of an Oxygraph-2k high resolution respirometer (Oroboros Instruments, Austria), containing 2 mL of MiR05 under constant stirring (750 rpm) at 15 °C (the same temperature used in whole-animal flow-through respirometry measurements). First, we assessed stable State 2 mitochondrial respiration rates stimulated with L-proline (10 mM). We used L-proline as a substrate because it was the only fuel that stimulated measurable O_2 consumption rates in tissue from both non-diapausing and diapausing beetles (SI, Fig. S7). After stable State 2 respiration rates were reached with the addition of L-proline, we added ADP (2 mM) and Mg^{2+} (5 mM) to stimulate State 3 respiration. We then added oligomycin (1 mg/mL in ethanol) to inhibit ATP synthase and estimate State 4 respiration followed by CCCP (1 mM) to uncouple electron transfer from O_2 consumption and measure Maximal Uncoupled mitochondrial respiration rates (Figure S2). We compared State 3 respiration rates using a one-way ANCOVA, with fresh flight

muscle mass as a co-variate, and analysed differences among treatment groups using a Tukey's HSD in R (R, version 3.3.2, R Core Team, Vienna, Austria).

Citrate synthase activity

We measured citrate synthase activity in flight muscle as citrate synthase activity is often used as a proxy for mitochondrial abundance (5). We included CPB from the following groups: non-diapause (control), exposed to diapause-inducing conditions for three, six, nine, 12, 15, and 20 weeks (emerged). We dissected flight muscle from beetles in each group directly into Ringer's solution (160 mM NaCl, 11 mM KCl, 8.4 mM $CaCl_2$, 5.9 mM $MgCl_2$, 5 mM HEPES, pH=7.0), then placed tissue into pre-weighed 1.7 mL microcentrifuge tubes which We flash-froze in liquid nitrogen vapor and stored at –80 °C until use in enzyme assays. On the day of enzyme assays, We added ice-cold homogenization buffer (20 mM Tris, 1 mM EDTA, 0.1 % Triton X-100, pH 7.2; 20:1, buffer volume to tissue mass) to each sample, and homogenized the tissue using a handheld electric homogenizer (VWR Pellet Mixer). We then centrifuged the homogenate for 5 min at 2000 × *g* at 4 °C and transferred the supernatant to two new tubes; one aliquot was used for citrate synthase enzyme activity, and the other for protein quantification.

We performed citrate synthase enzyme assays according to Mathers and Staples, 2016 (6). Briefly, We combined 2.5 µl of supernatant with 294.5 µl of citrate synthase reaction mixture (50 mM Tris pH 8.0, 1.5 mM Acetyl Coenzyme A, 1.5 mM DTNB) in wells of a 96-well assay plate and ran parallel reactions with and without the addition of 33 mM oxaloacetate. We measured absorbance at 412 nm at 10 s intervals for 5 min at 21 °C for each reaction on a Spectromax plate spectrophotometer (Molecular Devices, Sunnyvale, CA), and calculated citrate synthase enzyme activity from the difference between rates with and without oxaloacetate. We ran samples in triplicate, and calculated citrate synthase activity from the mean of triplicates. We standardized citrate synthase enzyme activity to total protein concentration in each sample, which we measured using a bicinchoninic acid assay (ThermoFisher Scientific, Massacheusetts, USA). We compared citrate synthase enzyme activities among groups using a one-way ANCOVA using protein content as a co-variate and compared differences among each treatment group using Tukey's HSD in R (R, version 3.3.2, R Core Team Vienna, Austria).

Fluorescence and electron microscopy

We used fluorescence microscopy to image nuclei in the flight muscle of control beetles and beetles exposed to nine weeks of diapause-inducing conditions (during diapause maintenance). We dissected flight muscle from beetles in each treatment into ice-cold 4 % paraformaldehyde and incubated overnight at 4 °C. We then embedded tissues into paraffin, cross-sectioned the paraffin blocks (5 µm sections), and mounted the paraffinized flight muscle sections on slides. We deparaffinized tissue sections in xylene, rehydrated them in 70 % ethanol, and stained for nuclei using DAPI (4',6-diamidino-2-phenylindole; 0.6 µM). We imaged slides with a Zeiss LSM 5 Duo Vario confocal microscope and ZEN Pro software (Carl Zeiss Microscopy GmbH, Jena, Germany).

We used transmission electron microscopy to visualize the structure and presence of mitochondria in flight muscle cells. We included beetles from the following groups: non-diapause (control), exposed to diapause-inducing conditions for six, nine, 12, 15, and 20 weeks. We dissected flight muscle from beetles in each group straight into ice-cold fixative (2 % glutaraldehyde, 2.5 % paraformaldehyde in 0.2 M sodium phosphate buffer, pH=7.4) and incubated the samples overnight at 4 °C. We washed tissues (1 × 5 min, 5 × 30 min) in double distilled water to ensure the removal of residual fixative, and stained tissue with 1 % osmium tetroxide on ice and in the dark for 45 min. Directly following osmium tetroxide staining, we washed tissues (1 × 5 min, 5 × 30 min) in double distilled water to ensure the removal of residual osmium tetroxide, and stained with 2 % uranyl acetate in the dark, overnight. We washed tissues again (1 × 5 min, 5 × 30 min) in double distilled water, and then serially dehydrated the tissue in acetone, and embedded tissues in Epin-Araldite resin (Electron Microscopy Sciences, Fort Washington, PA, USA), which we then polymerized at 60 °C for four days. We cut 0.5 µm sections and stained each section with 2 % uranyl acetate (20 min per section), immediately followed by Reynold's lead citrate (1 minute per section). We imaged sections at 19000× magnification with a Philips CM10 Transmission Microscope (Philips Electron Optics, Eindhoven, The Netherlands) equipped with an AMT Advantage digital imaging system and Hamamatsu Orca 2 MPx HRL Camera (Advanced Microscopy Techniques, Woburn, MA).

mRNA abundance quantification

We used quantitative real time PCR to measure changes in abundance of mitophagy and mitochondrial biogenesis-related transcripts. We included beetles from the following groups; non-diapause (control), exposed to diapause-inducing conditions for six, nine, 12, 15, and 20 weeks. We dissected ~5 mg of flight muscle from beetles in each treatment group directly into Ringer's solution (160 mM Nacl, 11 mM KCl, 8.4 mM $CaCl_2$, 5.9 mM $MgCl_2$, 5 mM HEPES, pH=7.0), placed tissue into pre-weighed 1.7 mL microcentrifuge tubes, flash froze tissues in liquid nitrogen vapor, and stored them at -80 °C until RNA extractions.

We extracted RNA using TRIzol (ThermoFisher Scientific, Mississauga, ON, Canada) according to the manufacturer's instructions, removed residual genomic DNA from the sample using DNAse (Quantabio, Beverley, Massachusetts, USA), and measured absorbance at 260 nm to determine the RNA concentration and quality using a Nanodrop spectrophotometer (ThermoFisher scientific, Mississauga, ON, Canada). The A_{260}/A_{280} of all RNA samples after DNAse reactions was between 1.8-2.0, indicating high quality RNA. We synthesized cDNA from 1000 ng of RNA using the iScript cDNA synthesis kit (Bio-rad Laboratories, Inc. Hercules, California, USA), and stored the cDNA in -20 °C until use. We diluted all cDNA to the same concentration prior to use in qPCR reactions. To amplify cDNA, we used SsoAdvanced Universal SYBR Green supermix (Bio-rad Laboratories, Inc, Hercules, California, USA) according to the manufacturer's instructions. Each qPCR reaction included a working concentration of 10 µM of forward and 10 µM reverse primer (final concentration of 0.4 µM), and 1000 ng cDNA, and we ran each reaction in triplicate using a Rotor-Gene Q real-time PCR cycler (Qiagen, Hilden, Germany).

We normalized transcript abundance in two ways; to two reference genes (*TBP1* and *EF1α*; See Table S1 for primer sequence information), and to internal calibrator samples consisting of cDNA synthesized from RNA extracted from fat body tissue in control beetles. We used these internal calibrator samples in each run to control for any inconsistencies among different qPCR runs. Finally, we calculated relative normalized transcript abundance using the comparative C_T method ($2^{-\Delta\,\Delta CT}$), which compared treated samples (those under diapause-inducing conditions) against the non-diapausing control (7). We compared comparative C_T values using a one-way ANOVA and compared differences among treatment groups using a Tukey's HSD test in R (R, version 3.3.2, R Core Team 2017 Vienna, Austria).

dsRNA production and RNA interference knockdown of Parkin

We designed and synthesized a dsRNA construct to target *Parkin*, and also synthesized a dsRNA construct complementary to *green fluorescent protein* (*GFP*), to inject as a negative control for off-target effects and should not target any endogenous insect mRNAs. We used E-RNAi (8) (https://www.dkfz.de/signaling/e-rnai3/) to design primers which could amplify either *Parkin* (NCBI: XM_023174278.1) from beetle cDNA or *GFP* (Genbank: U55762.1) from a pEGFP-N1 plasmid. Each primer contains a T7 promoter sequence on the 5' end, which is required for downstream dsRNA synthesis by a T7 RNA polymerase. We used these primers to generate templates for dsRNA from beetle cDNA and the pEGFP-N1 plasmid *via* PCR (GeneDirex Taq DNA polymerase; FroggaBio, Toronto, ON, Canada), according to the manufacturer's instructions.

We synthesized dsRNA using the MEGAScript RNAi kit (ThermoFisher Scientific, Waltham Massachusetts, USA) according to the manufacturer's protocols. Briefly, we transcribed *Parkin* and *GFP* amplicons from both 5' ends to single stranded RNA (ssRNA), annealed the complementary ssRNA molecules by heating them to 75 °C and allowing them to cool to room temperature and thus anneal to dsRNA, and performed a final nuclease digestion to remove residual DNA and ssRNA. We confirmed successful dsRNA synthesis by performing gel electrophoresis and observing bands at 484 bp and 411 bp for *parkin* and *GFP*, respectively.

We reduced the transcript abundance in diapausing beetles by injecting diapausing beetles with *dsParkin*, and injected a second group with *dsGFP* as a negative control. We injected beetles with a 10 µl Hamilton syringe (Hamilton Company, Reno, Nevada, USA) fitted with a 30 G needle, filled with 1 µg of dsRNA complementary to *parkin* or *GFP* in 5 µL 1× phosphate-buffered saline. To ensure we injected beetles with dsRNA prior to the peak expression of *Parkin* during diapause (nine weeks), we used beetles that had been in diapause-inducing conditions for seven weeks. We used qPCR to verify transcript knockdown and Western blot analysis to verify protein knockdown (as described below). We used the same individuals for qPCR and Western blot analysis. After injection we waited five days before dissecting ~5 mg flight muscle directly into Ringer's solution. Five days was the amount of time to reach maximal transcript knockdown in beetle flight muscle (Fig. S5). We then measured whole-animal metabolic rate, flight muscle mitochondrial respiration rate, citrate synthase enzyme activity and mitochondrial abundance in knockdown beetles 5 days post-injection.

Protein quantification by Western Blotting

To extract protein from flight muscle, we placed 200 µl of lysis buffer (2% SDS, 50 mM Tris, 1 mM PMSF, 1× protease inhibitor cocktail [Sigma Aldrich, St. Louis, Missouri, USA]) into tubes with tissue, sonicated samples 2 × 20 s with a handheld sonication probe (LabX, Ontario, Canada), and centrifuged them 5000 × *g* at 4 °C for 10 min. We reserved a 10 µl aliquot (diluted 10× in 90 µl lysis buffer) for protein quantification using a BCA protein assay kit (Thermo Scientific, Waltham, MA, USA) to determine the volume of extract containing 20 µg of protein.

We denatured protein extracts in 4×Laemmli Sample buffer at 100 °C for 5 min prior to loading (20 µg of protein/ well) in a 4-20% polyacrylamide TGX Stain-Free Gel (Bio-Rad, Mississauga, ON). We separated protein by electrophoresis at 120 V for 1.5 h in Tris-glycine-SDS running buffer (25 mM Tris, 192 mM glycine, 0.1% SDS). After electrophoresis, we activated gels on a ChemiDoc imaging system (Bio-Rad, Mississauga, ON) using UV light which allowed for total protein visualization for eventual standardization of Parkin protein abundance to total protein abundance. After gel activation, we immediately transferred proteins to a polyvinylidene fluoride (PVDF) membrane (Bio-rad, Mississauga, ON) at 100 V for 2 h at 4 °C. Immediately after transferring, we imaged the blot for total protein on a ChemiDoc imaging systems, washed the membranes 3 × 5 min in 1× TBS-T, and then blocked membranes at room temperature for 2 h with 5% bovine serum albumin (BSA) in 1× Tris-buffered Saline (TBS-T; 20 mM Tris, 143 mM NaCl, 0.05% Tween-20) under constant agitation. After blocking, we washed each membrane 3 × 5 mins with 1× TBS-T, and probed membranes with a custom *Leptinotarsa decemlineata* Parkin primary antibody (Life Tein Labs, 1:1000 in 0.05% BSA in TBS-T, antibody raised against *L. decemlineata* parkin sequence Accession ID: XP_0230300053) for 15 h at 4 °C under constant agitation. After primary antibody incubation, we washed membranes 3 × 5 mins in 1× TBS-T, and then incubated membranes with a secondary antibody (mouse anti-rabbit, 1:10000 in 5% BSA in TBS-T; Santa Cruz Biotechnology, California, USA) for 1.5 h at room temperature under constant agitation. Finally, we imaged membranes using the Biorad ChemiDoc system after incubating membranes in Pierce ECL Western blot substrate (Bio-rad, Mississsauga, ON).

Figures and Tables

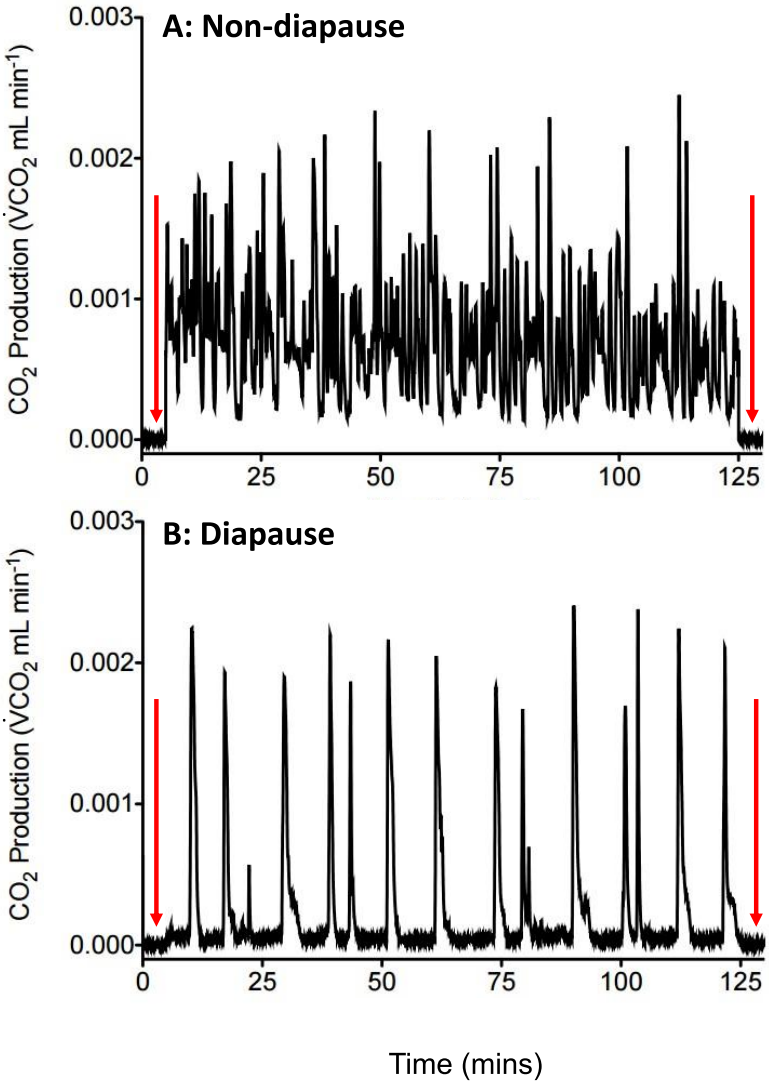

Fig. S1. Representative respirometry traces from Colorado potato beetles. CO_2 production ($\dot{V}_{CO2}$) in a (A) non-diapausing female (109.16 mg) and a (B) diapausing female (129.70 mg) measured at 15 °C. Non-diapausing beetles show patterns of continuous gas exchange, while diapause beetles show patterns of discontinuous gas exchange**.** Red arrows indicate baseline measurements taken in the first and last five minutes of the run (Supplementary Methods).

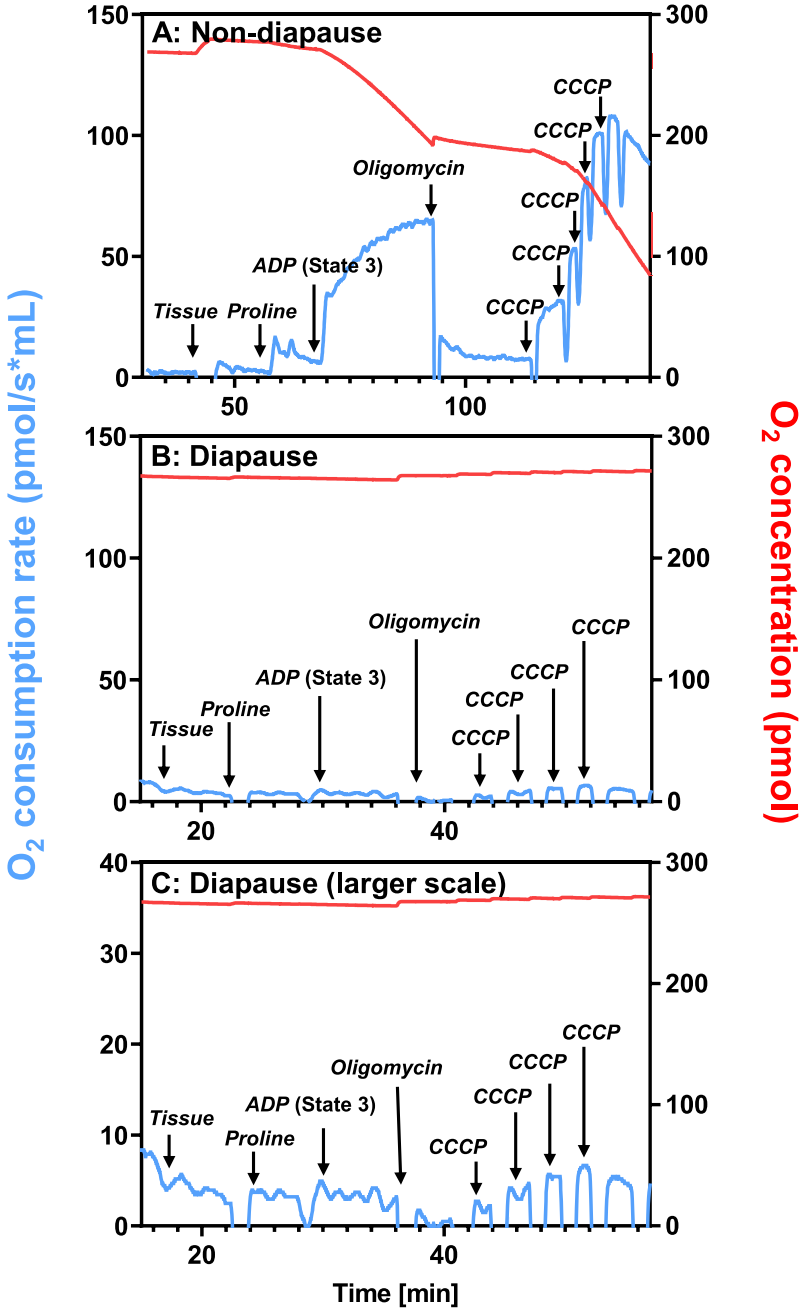

Fig. S2. Representative high-resolution respirometry traces from (A) non-diapausing (5.39 mg of tissue) and (B-C) diapausing (2.34 mg of tissue) flight muscle showing O_2 consumption rates (blue line) of permeabilized tissue and O_2 concentrations (red line) in the oxygraph chamber. (B) and (C) are the same trace, (C) is shown with a smaller scale. For details on substrate concentrations and our exact protocols see supplementary methods. First, we added pre-weighed permeabilized tissue into the oxygraph chamber, and waited for rates to stabilize. We then added saturating proline to stimulate State 2

respiration and waited for rates to stabilize. We then added saturating ADP to stimulate State 3 respiration and waited for those rates to stabilize. Finally, we added oligomycin followed by CCCP to inhibit ATP synthase and uncouple electron transport from ATP synthesis to measure uncoupled mitochondrial respiration rates. We added CCCP in a step-wise fashion until respiration rates plateaued. These data were collected from two separate runs, therefore the absolute time on the x-axis does not match up between panels.

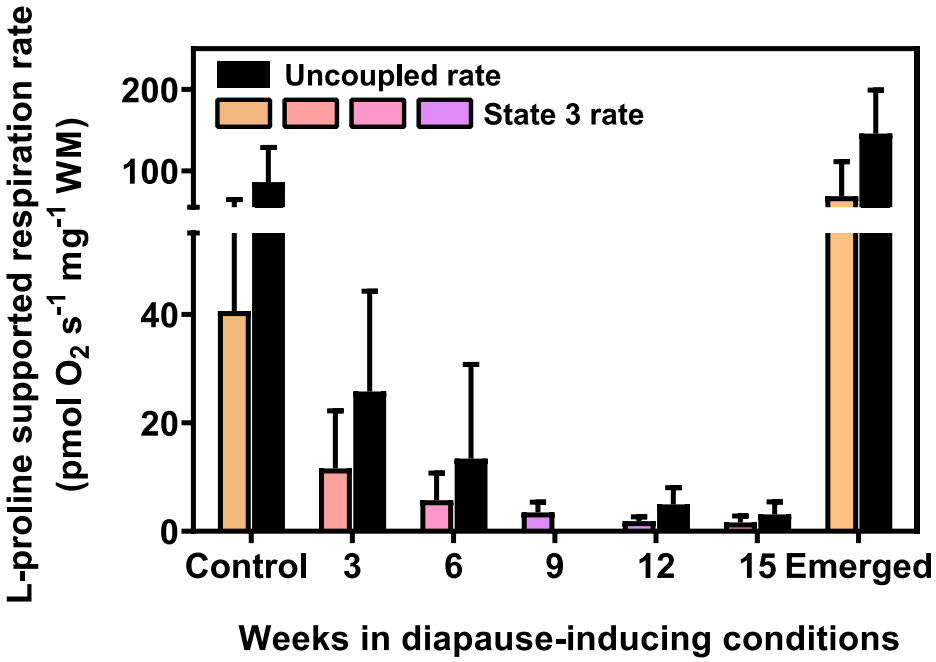

Fig. S3. State 3 (colored bars) and maximal uncoupled (black) mitochondrial respiration rates of beetles entering diapause (3-6), in diapause (9-15), and emerged from diapause. Colored bars are the same values as presented in Figure 1B, and black bars are the maximal uncoupled mitochondrial respiration rates associated with each colored State 3 mitochondrial respiration rate. Data show mean ±S.D. mitochondrial respiration rates.

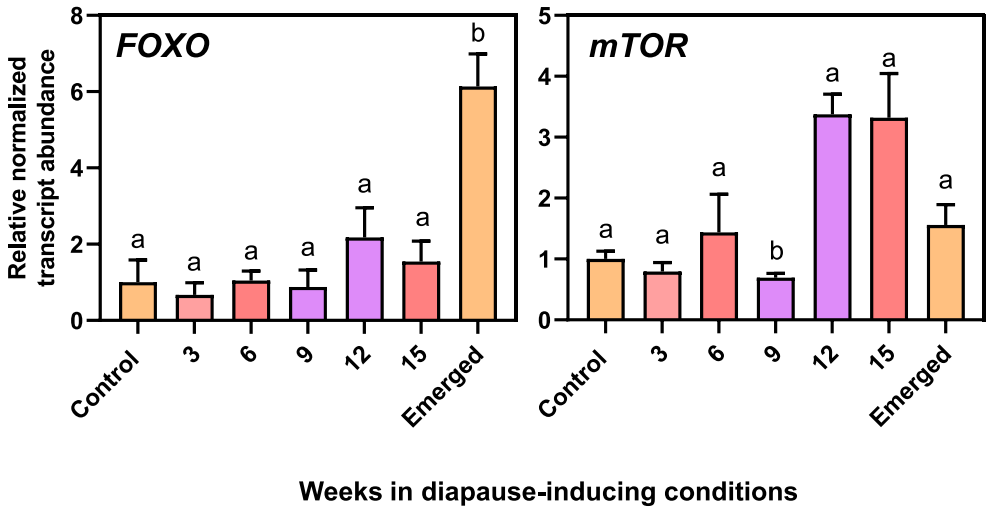

Fig. S4. Relative normalized transcript abundance of (A) *mTOR* and (B) *FOXO* in flight muscle of control beetles, and beetles exposed to three, six, nine, 12, 15, and 20 weeks of diapause-inducing conditions. Beetles at 20 weeks had emerged from diapause Expression values are normalized to control values and two reference genes according to the $\Delta\Delta C_t$ method (Supplementary Methods), and are plotted as mean ± S.D. Data were analyzed with a one-way ANOVA and difference letters denote significant differences among treatment groups ($p<0.05$). Statistics can be found in Table S2.

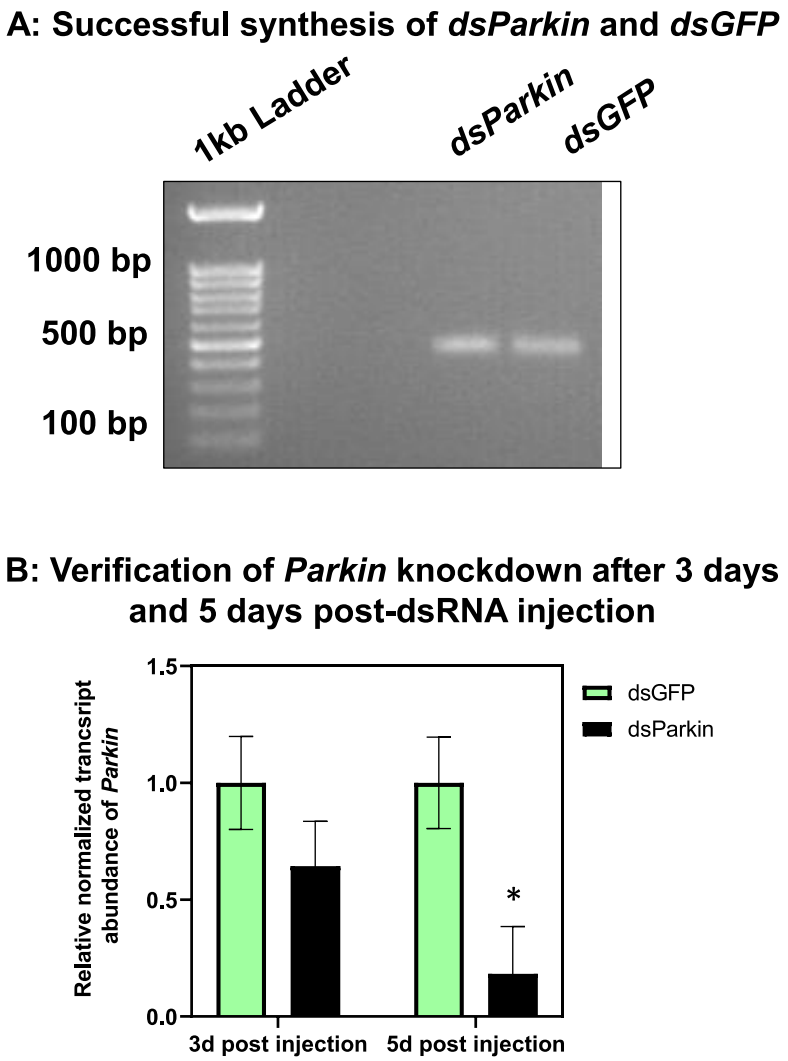

Fig. S5. (A) Successful synthesis of *parkin* and *GFP* dsRNA products at the expected size of 484 and 411 bp, respectively. (B) Verification of *Parkin* transcript knockdown three and five days post-dsRNA injection. We injected beetles exposed to diapause-inducing conditions for seven weeks with 1 ug of dsRNA complementary to either *parking* or *GFP* (n=3/treatment) and compared *parkin* transcript abundance after three of five days post-injection. Asterisk indicates significant differences between treatments within the same timepoint, statistics can be found in Table S1.

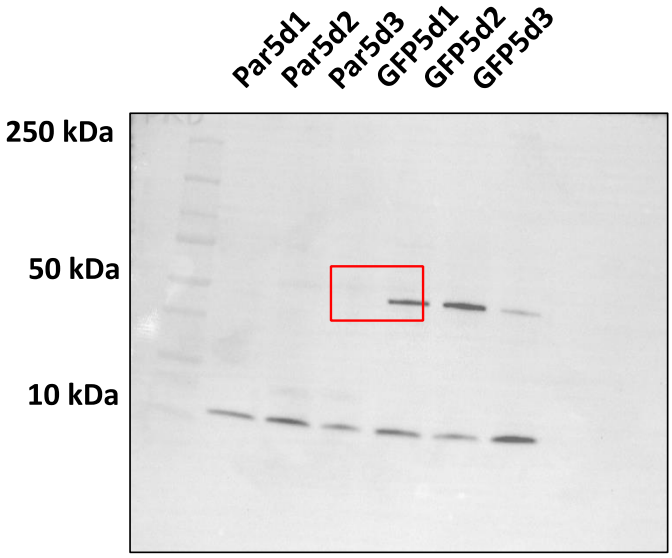

Fig. S6. Western blot composite image of colorimetric protein ladder and Parkin protein bands confirming protein knockdown of Parkin in diapausing beetle flight muscle. Each lane contains 20 µg of protein from flight muscle of the same individuals used for qPCR knockdown verification where the label "Par5d" describes individuals injected with dsParkin (n=3 beetles) and "GFP5d" describes individuals injected with dsGFP (n=3 beetles), and all flight muscle samples were collected 5 days after dsRNA injection; see supplementary data file 1 for qPCR data). The red box outlines lanes displayed in main text Figure 4. There is a non-specific band at ~10 kDa that is stable across all treatment groups.

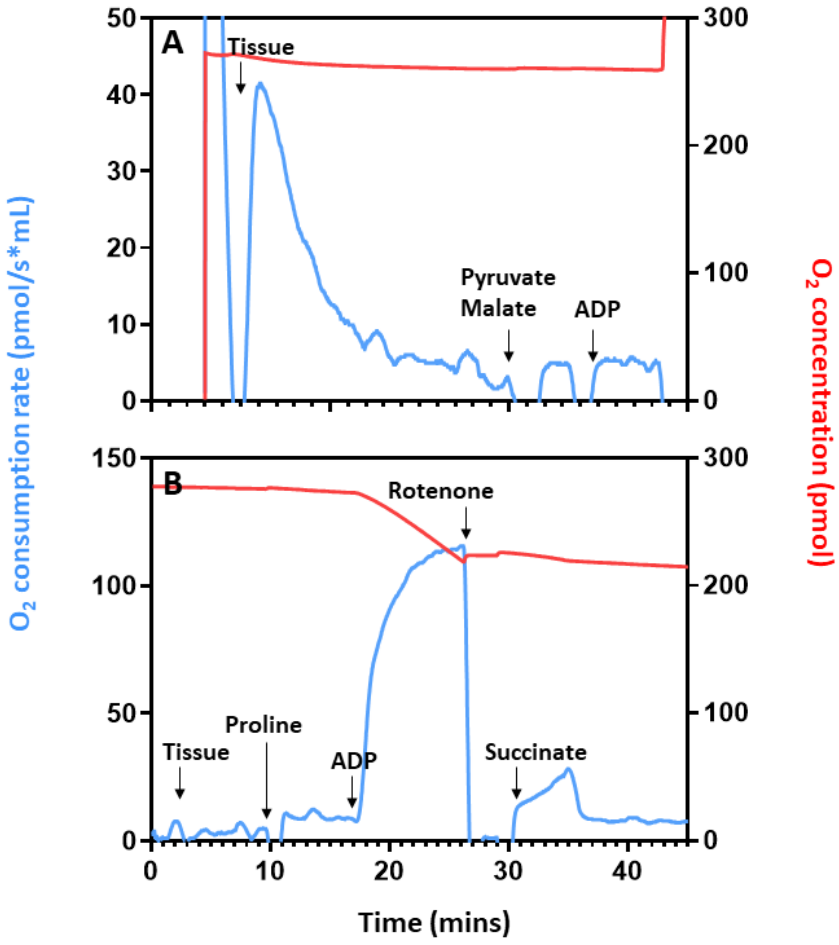

Fig. S7 Sample oxygraph traces testing complex I and complex II fuels. Both traces show that after the addition of a complex I fuels (pyruvate and malate; A) and complex II fuel (succinate; B) there is no appreciable increase in mitochondrial respiration rate, and that only the addition of proline stimulates substantial mitochondrial respiration. (A) Shows the addition of permeabilized flight muscle from a non-diapausing beetle, malate (2 mM), pyruvate (10 mM), and then ADP (2 mM) to stimulate State 3 mitochondrial respiration. (B) Shows the addition of permeabilized flight muscle from a non-diapausing beetle, proline (10 mM) and ADP (2 mM) to stimulate State 3 mitochondrial respiration, and then the addition of rotenone (0.5 µM) to inhibit respiration through Complex I, and then the addition of succinate (10 mM) to stimulate State 3 mitochondrial respiration through Complex II.

Table S1. Forward and reverse primer sequences for all genes of interest for *Leptinotarsa decemlineata*. Primers listed for mitophagy-related, mitochondrial biogenesis-related, and "other" were used for measuring transcript abundance of indicated genes of interest. Primers listed for dsRNA construct synthesis were used to amplify templates for double stranded RNA (dsRNA) synthesis. The 5' end of each primer used for dsRNA construct synthesis contains a T7 promoter which allowed RNA polymerase to bind to each primer and initiate dsRNA synthesis. Details on cycling conditions for all primers can be found in the methods.

Gene of interest	***Forward primer (5' to 3')***	***Reverse primer (5' to 3')***
Mitophagy-related		
Parkin	AAGCCTTGTCCGCAATGTAG	CACCAGTGAAATGCACATCC
PINK1	GTGTACGCGGGGAGATGTAA	GTCTGCCACCTTGGCTTTAT
ATG5	TTGATGGTTCCACGACTCAG	CACATCTCCTGGTCCGATTT
Mitochondrial biogenesis-related		
PGC1a	CAGGTTTGGCCCTATAACGA	CGACCTCCAAAGCTCAAGTC
NRF1	TCATACCGCTGATGCTGAAG	CACCAAGGAGGCCTTGTAGA
Other		
mTOR	TGAGACCACTATGGCTGACG	ACGACAACCAACTTCCAACC
FOXO	TGTCTCGGAAGGTCTCGATT	TTGCCCCAGTCAGGTTCTAC
Reference		
TBP1	ATGTCAAGCAGAAAGTCAAGAATCC	GCCGTAATATCCCTAACTCCCAAG
EF1a	CAGGGCAAGGTTTGAAAGATAA	CGTCTGCTTTGCGATTGAG
dsRNA construct synthesis		
Parkin	TAATACGACTCACTATAGTTTGCAAAAGTGGTGCATTC	TAATACGACTCACTATAGCTGCCAGAACTGTCTCTCC
GFP	TAATACGACTCACTATAGAGACACATGAAGCAGCACGACTT	TAATACGACTCACTATAGAGAAGTTCACCTTGATGCCGTTTC

Table S2. Summary of statistics for all relevant figures.

Experiment	**Figure**	**Statistic**	***P***
Metabolic rate	1A		
Treatment		$F_{6,34}$=107.72	<0.001
Mass		$F_{1,34}$=35.14	<0.001
Mitochondrial respiration rate	1B		
Treatment		$F_{6,31}$=20.78	<0.001
Mass		$F_{1,31}$=14.03	0.007
Citrate synthase activity	2A		
Treatment		$F_{6,44}$=21.02	<0.001
Protein content		F_{144}=0.69	0.41
Gene expression			
Parkin	3C	$F_{6,14}$=5.67	0.026
PINK1	3C	$F_{6,14}$=6.57	<0.001
ATG5	3C	$F_{6,14}$=28.51	<0.001
PGC1a	3C	$F_{6,14}$=3.16	0.036
NRF1	3C	$F_{6,14}$=25.47	<0.001
mTOR	S1A	$F_{6,14}$=4.45	0.010
FOXO	S1B	$F_{6,14}$=7.23	0.001
RNAi Knockdown verification	4	T_4=2.37	0.030
RNAi Metabolic rate	6A	T_7=1.93	0.040
RNAi Mitochondrial respiration rate	6B	T_6=1.31	0.240
RNAi Citrate synthase activity	5A	T_6=5.23	<0.001
RNAi Mitochondrial Density	5B	T_2=4.34	0.020

Dataset S1 (separate file). *"Reversible mitophagy_Supplementary_Dataset S1.xlsx"*
All experimental data in excel .xlsx format. See 'Read me' in the first tab of the datasheet for specific details.

Dataset S2 (separate file). "*Reversible mitophagy_Supplementary_Dataset S2.pdf"*
Sample raw electron micrograph images from all treatment groups saved in pptx format. See 'Read me' in file more details.

SI References

(1) J.E. Lebenzon, A.S. Torson, B.J. Sinclair, Diapause differentially modulates the transcriptomes of fat body and flight muscle in the Colorado potato beetle. *Comparative Biochemistry and Physiology D* **40**:100906 (2021).
(2) C.M. Williams et al., Thermal variability increases the impact of autumnal warming and drives metabolic depression in an overwintering butterfly. *PLoS One* **7**, e34470 (2012).
(3) A. Eigentler et al., Selected media and chemicals for respirometry with mitochondria and permeabilized cells. *Mitochondrial Physiology Network* **3**, 1-9 (2012).
(4) A.V. Kuznetsov et al., Analysis of mitochondrial function in situ in permeabilized muscle fibers, tissues and cells. *Nature Protocols* **3**, 965 (2008).
(5) S. Larsen et al., Biomarkers of mitochondrial content in skeletal muscle of healthy young human subjects. *Journal of Physiology* **590**, 3349-3360 (2012).
(6) K.E. Mathers, J.F. Staples, Saponin-permeabilization is not a viable alternative to isolated mitochondria for assessing oxidative metabolism in hibernation. *Biology Open* **4**, 858-864 (2015).
(7) K.J. Livak, T.D. Schmittgen, Analysis of relative gene expression data using real-time quantitative PCR and the $2^{-\Delta\Delta CT}$ method. *Methods* **25**, 402-408 (2001).
(8) T. Horn, M. Boutros, E-RNAi: a web application for the multi-species design of RNAi reagents—2010 update. *Nucleic Acids Research* **38**, W332-W339 (2010).